Chemical Physics Letters 769 (2021) 138401

Contents lists available at ScienceDirect

Chemical Physics Letters

journal homepage: www.elsevier.com/locate/cplett

Research paper

Synthesis and characterization of an industrially significant ionic liquid and its inclusion complex with β-cyclodextrin and its soluble derivative for their advanced applications

Raja Ghosh [a], Niloy Roy [b], Subhadeep Saha [c], Samir Das [b], Biraj Kumar Barman [d], Debadrita Roy [b], Vikas Kumar Dakua [e], Mahendra Nath Roy [e,*]

[a] Department of Chemistry, Sripat Singh College, Jiaganj, Murshidabad, WB 742123, India
[b] Department of Chemistry, University of North Bengal, Darjeeling 734013, India
[c] Department of Chemistry, Government General Degree College, Pedong, Kalimpong 734311, India
[d] Department of Chemistry, Parimal Mitra Smriti Mahavidyalaya, Malbazar, Jalpaiguri, WB 735221, India
[e] Department of Chemistry, Alipurduar University, Alipurduar, WB 736122, India

ARTICLE INFO

Keywords:
1-Dodecyl-4-methylpyridinium iodide or **DMPI**
Hydroxypropyl-β-cyclodextrin or **HP-β-CyD**
Inclusion complex
Job plot
Scanning electron microscopy or **SEM**
Ionic liquid based surfactants or **ILBS**

ABSTRACT

Thermochromic also solvatochromic ionic liquid surfactant was synthesized and characterised. The surface activity, size and stability were estimated by surface tension, SEM and DLS techniques. Inclusion complexes construction of the synthesized compound with the β-cyclodextrin and derivative was explored by various techniques. Conductance, surface tension trial & Jobs obtained from the UV–vis spectra proved the formation of 1:1 inclusion complexes between the surfactant and cyclodextrins. Binding constants and thermodynamic parameters of the inclusion of the guest DMPI with both hosts were determined with UV–vis and sophisticated fluorimetric analysis. Anti bacterial properties of DMPI and its both inclusion complexes were analyzed.

1. Introductions

Ionic liquids (ILs) are basically organic nano structured molten salts having cationic organic part and anionic inorganic or organic counterpart [1] ILs have large diversity of unique physical and chemical characters such as non-flammability, minor vapour pressure, ability of dissolving large variety of compounds, high electrical conductivity, widely recognized liquid range etc. [2–6].

The all-round and useful properties of ILs have been documented in the current millennium; this led to a speedy escalation in the number of basic research on ILs. Eventually, it was recognized that these properties should also be applied to compounds that carry lengthy hydrocarbon chains, i.e., compounds with surface activity [7,8].

β-cyclodextrin (β-CyD) is made up of glucopyranosyl units attached to α-1,4-glycosidic linkages. β-CyD has broad uses in biomedical, pharmaceutical and other field of sciences e.g. for its good bioavailability, safety, stability, as a solubility enhancer and efficient carrier of the suitable guest molecule [9,10].

Though β-cyclodextrin has originality in its application but suffers from some demerits like low solubility and behave like nephrotoxins. It is crucial to use as small amount of CyDs as likely in pharmaceutical and new formulations. In this respect, aqueous solubility of α-CyD and γ-CyD is more useful than β-CyD [11,12]. Solubility of β-CyD can be considerably increased by derivatization. Hydroxypropyl-β-Cyclodextrin (HP-β-CyD) is one of the main persistent pharmaceutical formulations. HP-β-CyD like other cyclodextrins can enhance the solubility of sparingly and poor soluble drug or other molecular guest by the formation of inclusion complexes more efficiently. HP-β-CyD is with negligible amount of toxicity and may be useful in the improvement of parenteral administration of less soluble drugs [13,14].

HP-β-CyD is an alternate of α, β and γ-cyclodextrin, with better water solubility and may also be toxicologically benign. It is promptly and

Abbreviations: CyD, Cyclodextrin; CyDs, Cyclodextrins; DMPI, 1-Dodecyl-4-methylpyridinium iodide; IC, Inclusion complex; ICs, Inclusion complexes; ID, 1-Iodododecane; MPy, 4-methylpyridine; DLS, Dynamic light scattering; DSC, Differential scanning calorimetry; EDS, Energy Dispersive X-Ray Spectroscopy; FTIR, Fourier-transform infrared spectroscopy; HP-β-CyD, Hydroxypropyl-β-cyclodextrin; ILs, Ionic liquids; ILBS, Ionic liquid based surfactants; SEM, Scanning electron microscopy.

* Corresponding author.
E-mail address: mahendraroy2002@yahoo.co.in (M. Nath Roy).

https://doi.org/10.1016/j.cplett.2021.138401
Received 8 November 2020; Received in revised form 22 January 2021; Accepted 29 January 2021
Available online 2 February 2021

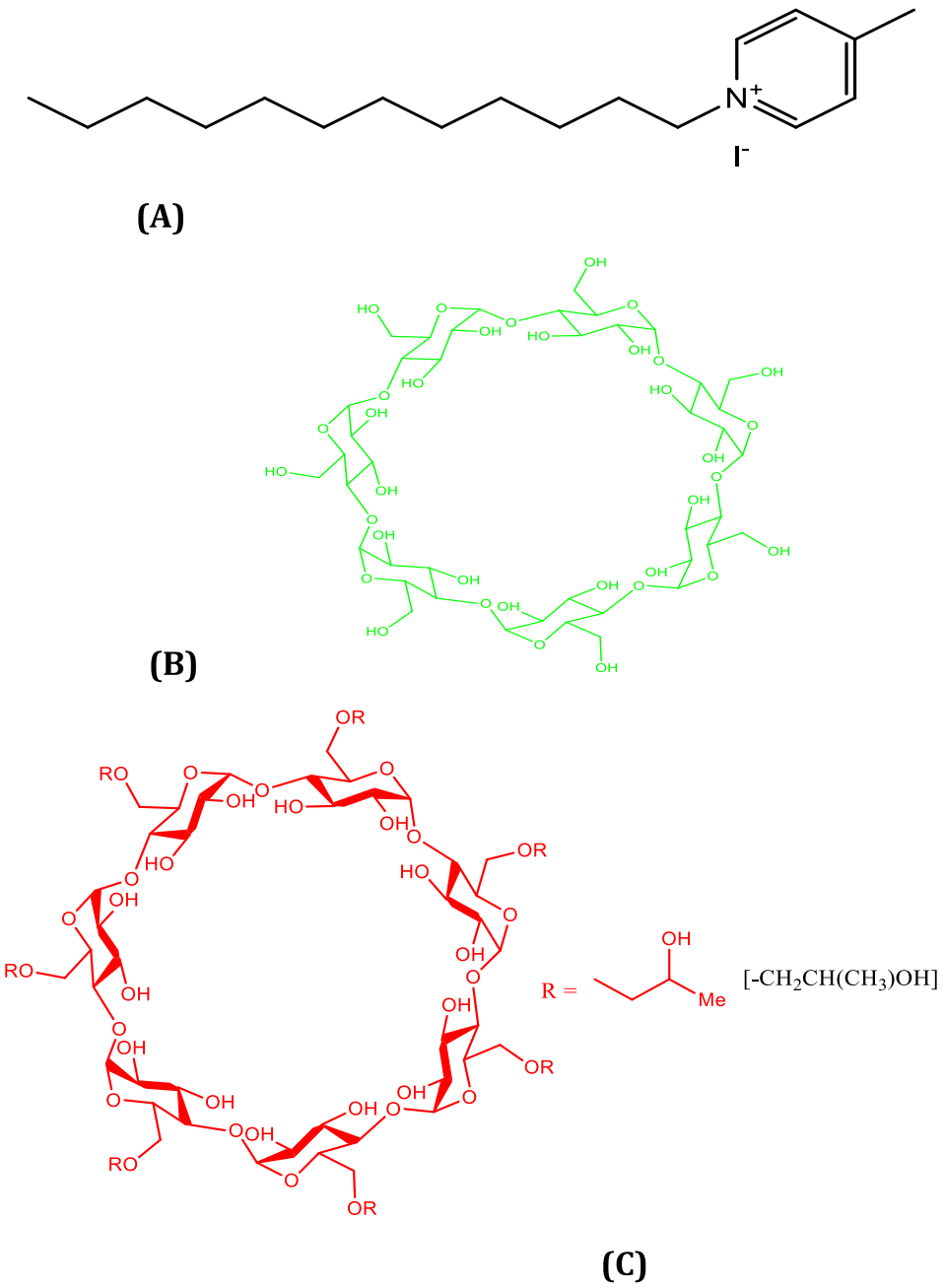

Scheme 1. Molecular structure of (A) DMPI (B) β-CyD & (C) HP-β-CyD.

about entirely cleared from body though systemic passage by the kidneys after intravenous booster, and is cleared from the lung by being absorbed into the total circulation with subsequent running in an aerosol [15–17]. Amongst these cyclodextrins, β-CyD and its hydrophilic (hydroxypropyl) derivative, such as HP-β-CyD are the primary choices as of their appropriate cavity sizes and modest rate [18].

Till now the study on the inclusion phenomenon between pyridinium ionic liquid based surfactant (ILBS) and β-CyD or specially its hydroxypropyl derivative is comparatively rare in the literature. The inclusion phenomena of cyclodextrin has been studied extensively, however less often with ILBS, moreover very few technique like capillary electrophoresis etc were employed to explore the inclusion phenomena [19,20]. 1-Dodecyl-4-methylpyridinium iodide was synthesized using simple refluxing technique and characterized by UV–vis, FTIR, FTNMR, and LC-MS techniques.

Host-guest inclusion mechanisms of the synthesized product were studied with the β-CyD and its hydroxypropyl derivative. The stoichiometry of the host guest supramolecular inclusion complex with β-CyD was studied using conductivity, surface tension and further by Job plot derived from UV–vis study. Thermodynamic parameters were also derived by employing UV–vis and fluorimetric techniques. FTIR & FTNMR was employed to know about the successfully included part of the host. Zeta potential of the guest was obtained by Dynamic Light Scattering (DLS). Change in the surface morphology and size was checked by SEM (scanning electron microscopy) and DLS size measurement. Anti bacterial study of DMPI and its one inclusion complex were performed and compared with the DMPI (see Scheme 1).

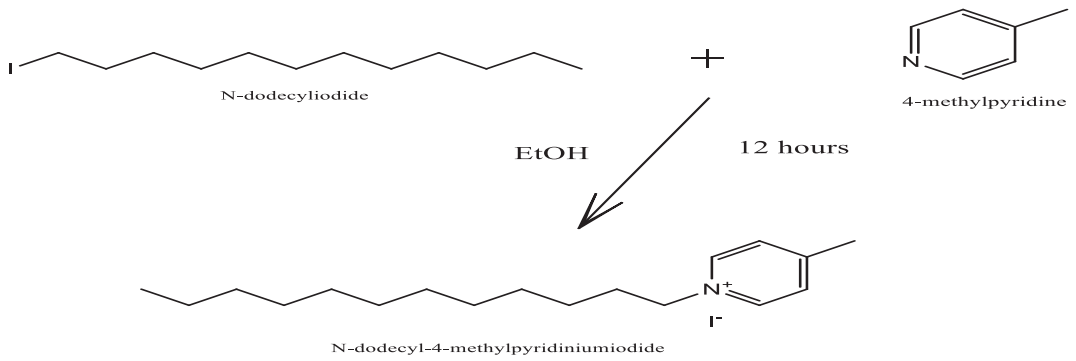

Scheme 2. Synthesis of DMPI.

2. Experimental section

2.1. Materials

4-Methylpyridine (MPy) and 1-iodododecane (ID) were used for synthesis as precursors. Double distilled water with specific conductance ~ 1.1 μScm^{-1}, pH ~6.9–7.0 was used for all experimental purposes. The source and purity of the chemicals have been given Table S.1.

2.2. Preparation of the guest

Before starting the synthesis, solubility of used precursors MPy and DI were precisely checked in different solvents and finally EtOH was selected as solvent. MPy and DI were taken in (1: 1.2) molar ratios in ethanol and refluxed for 12 h. The used solvent (EtOH, boiling point 78.37 °C or 351.37 K) was removed using rotary evaporator connected to vacuum pump by maintaining required temperature. The product was washed with PET ether for several times. To remove the waxy nature, the treated product was washed by diethyl ether 20 times. The purified product obtained was tested by TLC and discrete spot was found in comparison to the both the precursors. The product was dried, stored in dark place and vacuum desiccators for 72 h. The melting point of the sample was approximately 317 K. The melted sample was crystallized rapidly upon cooling. During the month of October/November needle like crystal formation from the product was spontaneous. Negative solvatochromism (blue shift with increasing solvent polarity) was shown by sample and the colour was changed from bright yellow to light green from THF to H_2O (order of polarity) respectively. Thermochromism was also visible distinctly in the sample. The colour of the sample was changed straw to yellowish above 317 K (see Scheme 2).

2.3. Apparatus and procedure

FTIR spectra were recorded in KBr pellets using PerkinElmer FTIR spectrometer (RX-1) operating in the region of 4000–400 cm^{-1} at ambient temperature. The software connected with the instrument was PerkinElmer precisely version 5.3 (Copyright 2005 PerkinElmer, Inc). The pellets formed manually. Humidity during experiments was approximately 45% [21,23].

^{1}H Nuclear magnetic resonance (NMR) was performed in Bruker AVANCE spectrometer operating at 300 MHz frequency. 2D ROESY spectra were carried out using 400 MHz Bruker AVANCE NMR spectrometer. The respective solutions were made in D_2O, data was reported as a chemical shift [10,22,23].

UV–vis spectra were recorded on Agilent 8543 spectrophotometer, with an uncertainty of wavelength resolution of ±1 nm. The measuring temperature was controlled by an automated digital thermostat of Julabo F32 [24]. The spectra were obtained with UV–vis ChemStation software (Revision B.04.02 [63], Copyright© Agilent technologies 2001–2011). The spectral scans were taken within range from 190 to 1200 nm.

The conductance measurements were performed in Mettler Toledo Seven Multi conductivity meter with uncertainty 10 μS cm^{-1} (Cell constant of about 0.1 ± 0.001) cm^{-1}. Solutions temperature was maintained to within (298.15 ± 0.01) K using Brookfield Digital thermostat bath (TC-550). 0.01 M aqueous KCl solution was used for cell calibration. The uncertainty in temperature was ±0.01 K [25].

Surface tension experiments were carried out by a platinum ring detachment method using a Tensiometer (K9, KRÜSS, Germany) at the experimental temperature. The accuracy of the surface tension measurement was within ± 0.1 mN m^{-1}. The constant temperature was maintained during the experiments with Remi ultra thermostat (CB-700) with precision 0.1 K.

Refractive index (RI) for DLS was measured with the help of a digital refractometer of Mettler Toledo Refracto 30GS. The light source was LED, λ = 589.3 nm. The refractometer was calibrated using distilled water, and calibration was checked after every measurement. The uncertainty of the measurement was ±0.0002 units [26].

Steady-state fluorescence emission study was carried out in bench top spectrofluorimeter from photon technologies international (Quantamaster-40). The software used was Felix-Gx software and Xenon lamp was used as the source of radiation for steady state fluorescence experiments (version 2.0) [22]. The samples were taken in a quartz cuvette of optical path length 1.0 cm [27].

Dynamic Light Scattering (DLS) was performed using a Zetasizer Nano ZS90 ZEN3690 light scattering apparatus (Malvern Instruments Ltd., Malvern, UK having the He-Ne laser of 632.8 nm, 4 mW) at a scattering angle of 90°. The temperature was fixed within the range of 293 K to 313 K [28]. Gas chromatography mass spectrometry (GC–MS) measurement was done in the Thermo Scientific (TRACE 1300) gas chromatography ISQ QD Mass spectrometer with data system is a high resolution and double focusing instrument.

Scanning electron microscope (SEM) instrument used was of Jeol JSM-IT 100, connected with EDS compartment with detector input area of 20 mm^2. Microanalysis was performed by an Oxford INCA energy dispersive spectrometer (EDS) connected to the SEM. All photography was taken & initially analyzed by InTouchScope (Version 1.060) software. Samples of DMPI, β-cyclodextrin, Hydroxypropyl β-CyD and their inclusion complexes were mounted onto aluminium stubs and sputter-coated with a gold layer of about few millimetres. These samples were analyzed by an energy dispersive X-ray spectroscopy. Experimental conditions involved 15 kV at low vacuum (30 Pa), current 8–10nA, beam

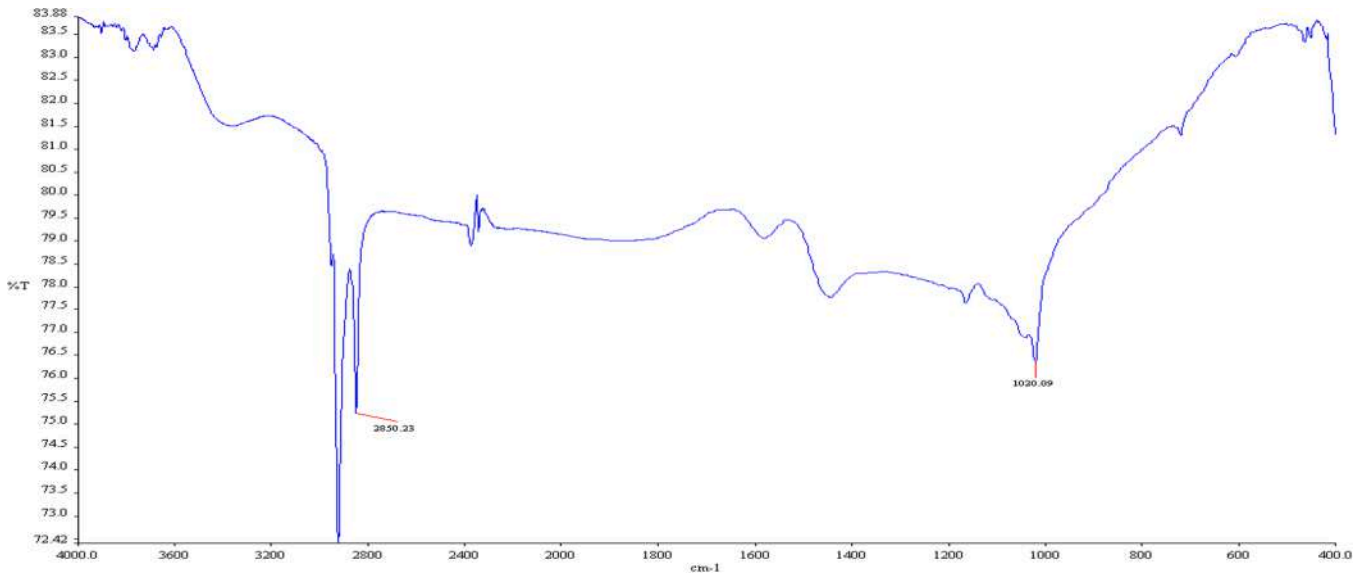

Fig. 1a. FTIR spectra of n-dodecyl iodide (one of the precursor).

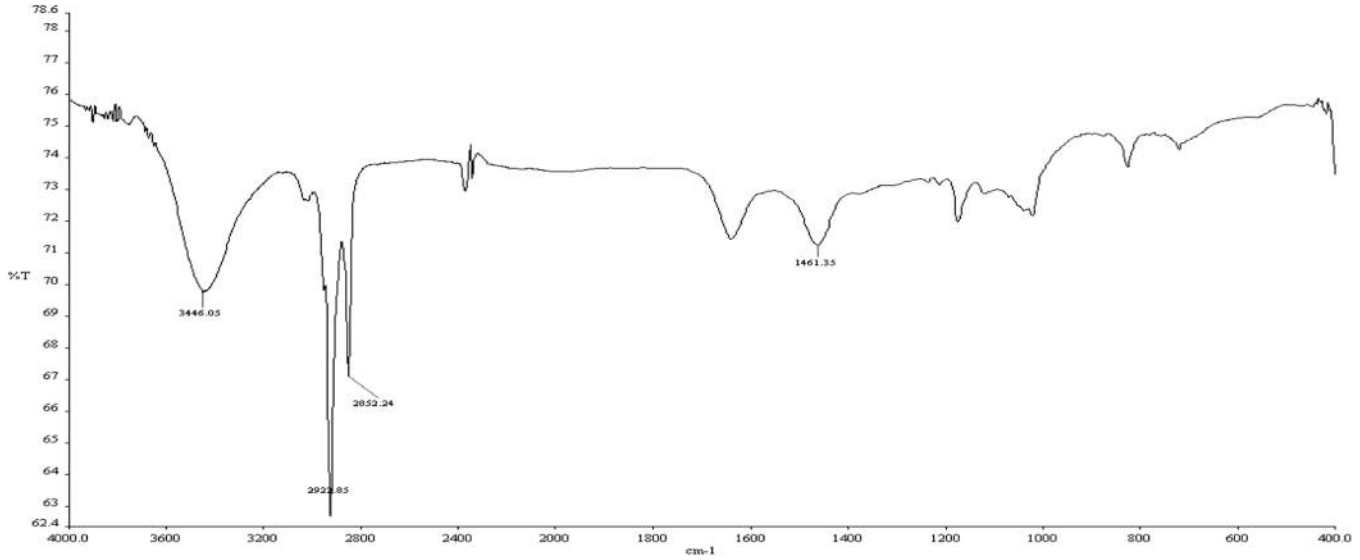

Fig. 1b. FTIR spectrum of pure DMPI (Product).

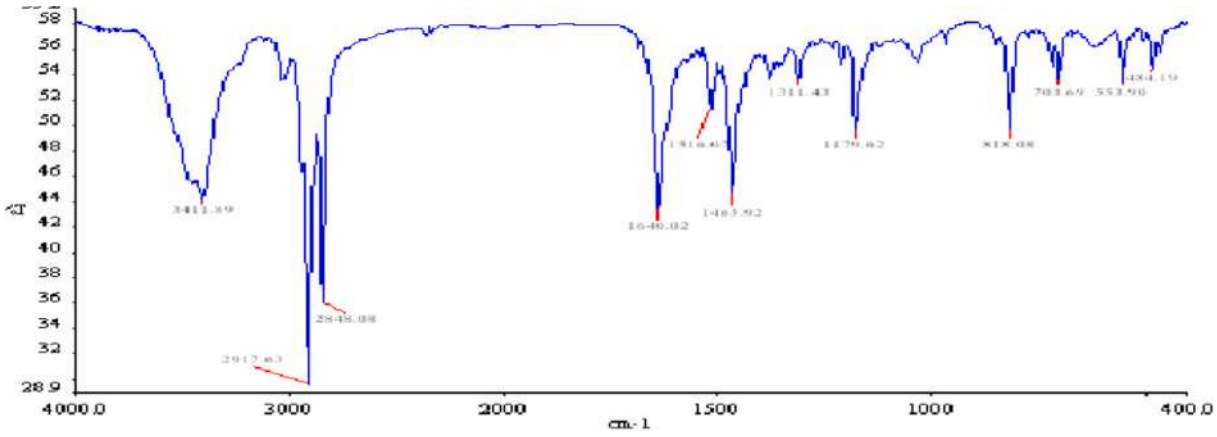

Fig. 1c. FTIR spectra of DMPI Crystalline (Product).

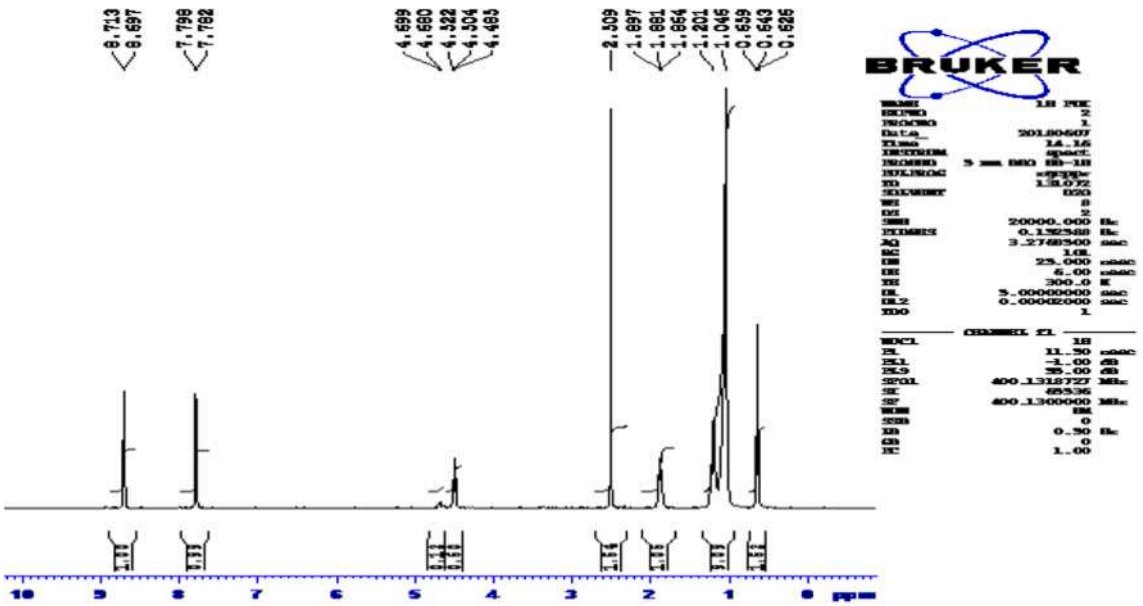

Fig. 2a. FTNMR spectrum of pure DMPI (^{1}H).

diameter 6 μm using a backscattered electron detector [17].

DSC experiment was done in nitrogen atmosphere by Pyris 6 DSC instrument, (Software: Pyris Manager software version 07.00.00.). Heating rate for the instrument was 2 K/min with equal amount of sample in each case.

2.4. *Characterization: spectroscopic*

2.4.1. *FTIR analysis*

The obtained infrared frequencies of the different bonds of functional groups of both the precursor (Fig. 1a) and product i.e. DMPI have been shown (Figs. 1b and 1c, & Fig. S.1) within the range of 400–4000 cm^{-1}. The broad band at 3446 cm^{-1} is ascribed to bond stretching of quaternary amine (3330–3450 cm^{-1}) like structure of dodecylpyridinium ring. Peak at 3012 cm^{-1} is due to aromatic —C—H bond vibrations of pyridinium ring. The peaks with wave numbers 2944 cm^{-1} and 2852 cm^{-1} of the aliphatic asymmetric and symmetric (—C—H) stretching vibration is owing to the methyl group (—CH_3). The peaks with wave number 2923 cm^{-1} and 1450 cm^{-1} are due to symmetric stretching and bending frequencies respectively of —CH_2— group. The —C═C— bond of pyridinium ring have absorption peak at 1630 cm^{-1} due to stretching vibration [22,29–34]. FTIR spectrum of the DMPI in methanol appears with broad peaks due to probable H-bonding interaction among the substrate & solvent. This spectrum also justifies the structure of DMPI except the exceptions of peak broadness. (Fig. S.1)

2.4.2. *NMR analysis*

The obtained product was characterized by ^{1}H NMR spectroscopy using either D_2O or D_2O + $CDCl_3$ (minor amount) mixture as solvent for the determination of molecular structure. The ^{1}H NMR spectra data are

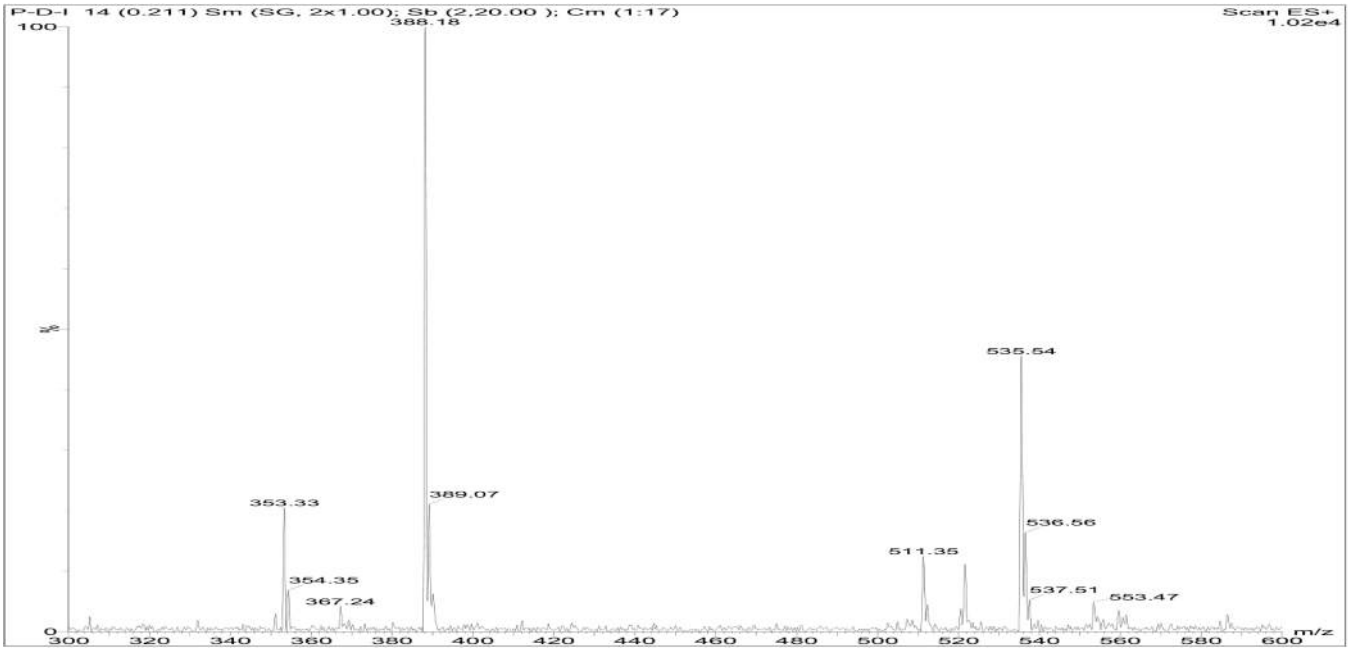

Fig. 2b. Mass spectrum of DMPI (Magnified) in CH_3CN.

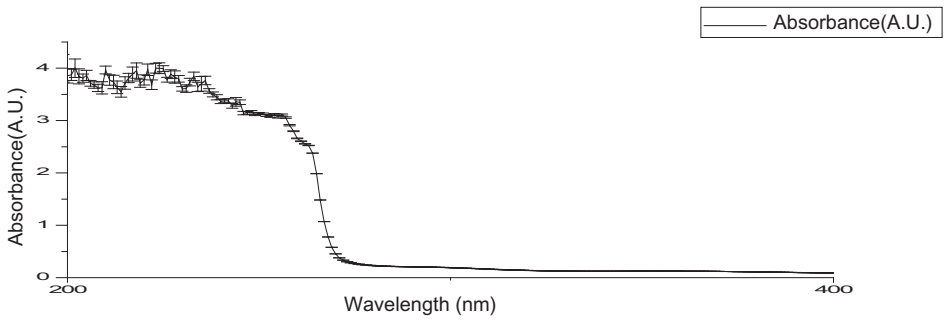

Fig. 3a. UV–vis spectrum of 50 μM crude DMPI in water at 298 K (Plot with standard deviation data as Y error).

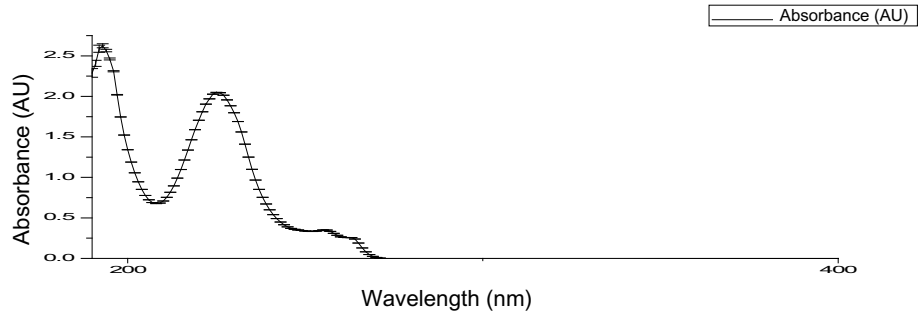

Fig. 3b. 50 μM IC of DMPI & HP-b-CyD in water (Plot with standard deviation data).

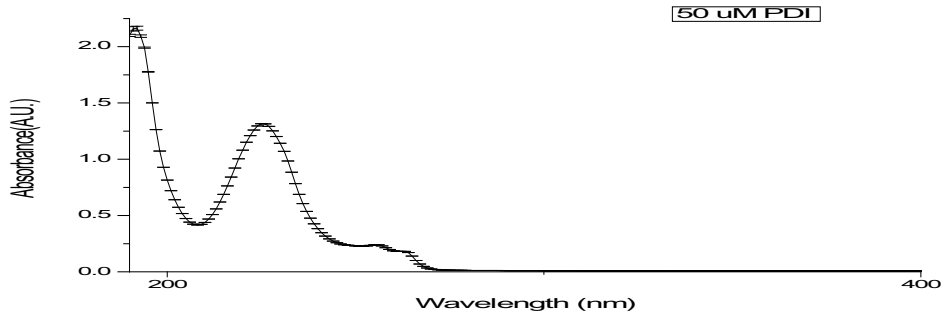

Fig. 3c. 50 μM DMPI at 298 K in water (Plot with standard deviation data).

shown in Fig. 2a, S.2, S.3. (a & b) & S. (4. & 5) in ppm (δ) from the internal reference (D_2O: δ 4.79 ppm and $CDCl_3$: δ 7.26 ppm wherever applicable) in determining the proton chemical shifts.

The results of ^{1}H NMR of DMPI are given as follows:

^{1}H NMR, DMPI (400 MHz, D_2O+ $CDCl_3$): δ **8.713–8.697** (d, 2H, J = 6.4 Hz) N(C**H**)$_2$ moiety of pyridinium ring, **7.798–7.782** (d, 2H, J = 6.4 Hz), N(+)CC(C**H**)$_2$ of pyridinium ring, **4.699–4.680** (H1, 7H, suppressed solvent peak, J = 7.6 Hz), **4.522–4.485** (t, 2H, NC**H**$_2$, J = 7.4 Hz), **2.509** [s, 3H, —C**H**$_3$ group para to N(+)], **1.897–1.864** (t, 2H, N(+)CC**H**$_2$, J = 6.6 Hz), **1.201–1.046** (m, N(+)CC(C**H**$_2$)$_9$, 18H), **0.659–0.626** (m, 3H, N(+)C$_{11}$C**H**$_3$).

Table 1
Solubility of **DMPI** in different solvents.

Solvent	Hexane	THF	EtAc	$CHCl_3$	DCM	DMSO
Solubility	x	✓	✓	✓	✓	✓
Solvent	**CH_3CN**	**C_2H_5OH**	**CH_3OH**	**Water**	**PET ether**	**Diethyl ether**
Solubility	✓	✓	✓	Slightly dispersed	x	x

2.4.3. GC-Mass spectrometry analysis

Gas chromatography mass spectrometry was performed in CH_3CN solvent. One of the important peaks was obtained at mass correspond to 391.33u. This confirms the formation of desired compound. The peak at 155 was due to the formation undecyl cation. GC–MS was shown in the figure Fig. S.6. Surface active compounds usually repress the mass spectra and the product which will be used as guest in subsequent part i. e. DMPI is itself surface active [22]. Mass spectrometric (In the -ve mode) result showed expected molecular ion peak at mass correspond to 388.18 u. (The approximate molecular weight of the analyte was 389.16u (Fig. 2b) [35–37].

2.4.4. UV–vis spectra analysis

n-π^* transition usually appear λ(nm) beyond 273, so we can belief that in DMPI no **n**-π^* is possible. The structure of the DMPI further make the supposition cleared that there was no **n**-π^* transition [38,39]. Pyridinium ring have three conjugated double bonds. It is expected that UV–vis band owing to π-π^* transition of the molecule. Two number of UV band appeared at 222 & 254 nm. (Fig. 3a, Fig. 3b and Fig. 3c) The band of 222 nm was much more intense than the 254 nm band. All 3 spectra were taken in room temperature. In Fig. 3b. IC DMPI shown enhance intensity in the presence of HP-b-CyD (As IC in water)

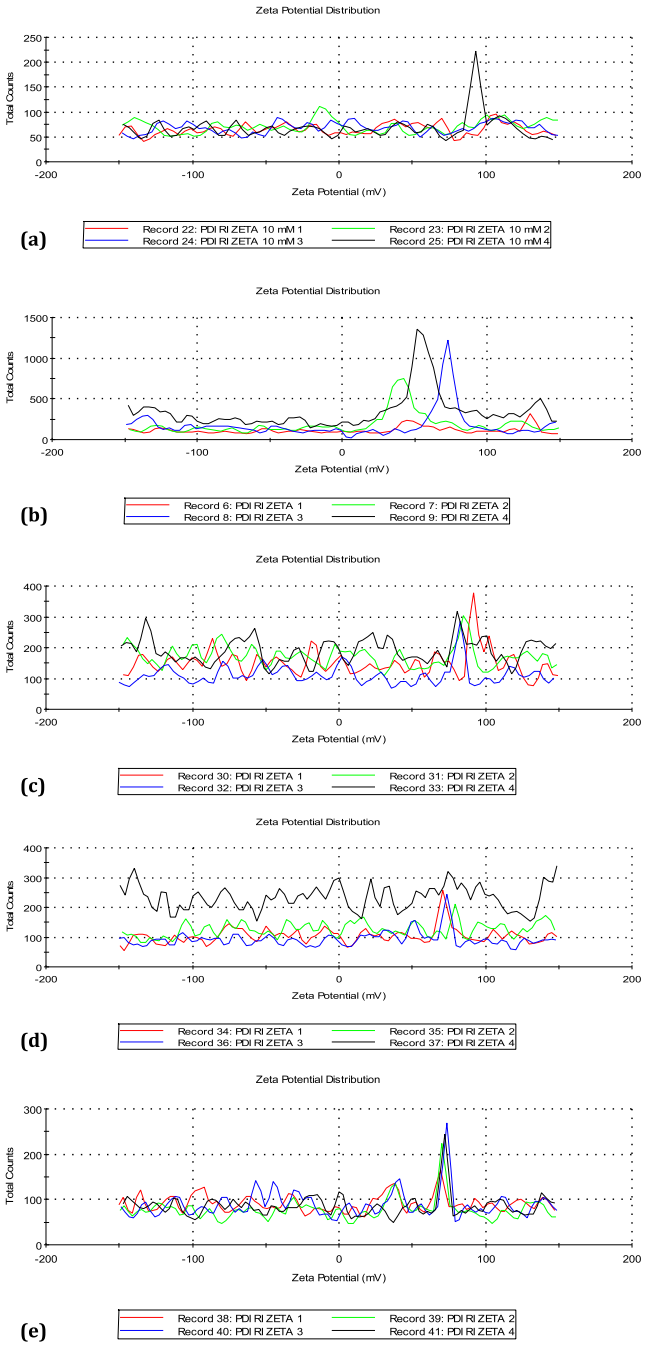

Fig. 4. (a)–(e): Zeta(ζ) potential distribution of 10 mM DMPI at 5 different temperatures (293 K, 298 K, 303 K, 308 K & 313 K respectively) in aqueous solution.

compared to in Fig. 3c. cyclodextrin's hydrophobic cavity offers a shielding environment which can guard the excited singlet species from gradual quenching and non radiative decay process occurring in solution.

3. Results and discussion

3.1. Investigation of physicochemical properties of DMPI

3.1.1. Solubility test

The compound was soluble in the different organic solvent and shown enhanced water solubility compared to both the precursors. The product's solubility test was performed qualitatively (see Table 1).

3.1.2. From DLS; Zeta potential

The Zeta-potential measurement is a key factor to understand stability of colloidal particles in aqueous solutions [40,41]. From the Zeta potential distribution graph [(Fig. 4a–e–, tab S. 2 (a)–(c) to tab. 6. (a)–(c)] (Total counts vs. Zeta potential in miliV) it was quite clear that DMPI has either significant positive or negative value of potential. So Zeta potential values validate about the stability of aqueous colloidal system [42,43].

4. Inclusion complex & inclusion mechanism:

4.1. Preparation of inclusion complex

We prepared the solid ICs (DMPI + β-CyD and DMPI + HP-β-CyD) in 1:1 M ratios. In each complex, 6.0 mM of CyDs and 6.0 mM of HP-β-CyDs were separately prepared in 20 mL of water each and stirred for 4 h. Then, the aqueous solution of DMPI was added drop wise to the both aqueous solution of CyDs. The resulting mixture was then stirred for 36 h at 318–323 K and filtered at this temperature. Both the resulting mixtures were then slowly cooled down to 278 K and held at this temperature for 8 h. Finally the solutions were filtered to obtain white powder, which was washed with water and ethanol respectively and dried in air. The yields of the solid inclusion complexes were 86% and 90% for TgCl + HP-β-CyD and TgCl + β-CyD respectively.

4.2. From specific conductance

The plot of conductance of DMPI with respect to the concentration for β-CyD & HP-β-CyD has shown in Fig. 5a, have a distinct break point at around 3.00 mM concentration of HP-b-CyD & b-CyD. There was only one break point, suggest the host guest ratio of 1:1 in inclusion complex in solution. The concentration correspond to the break point is less than the ideal concentration of 1:1 inclusion (i.e. 5 mM) as there may be less concentration of monomer molecule of ionic liquid surfactant DMPI due to its aggregation in the surface of the solution [22]. The concentration of the inclusion complexes (In dynamic equilibrium) in water should be around 3.00 mM initially. This 3.00 mM concentration should increase gradually as supramolecular hydrophobic interaction is stronger than hydrophobic interaction inside the micellar core [22].

4.3. From UV–Vis spectroscopy: Job plot:

A fit and successful method for identify the stoichiometry of host and guest in inclusion complexes is Job's method, usually known as the continuous variation method [44,45].

We employed the absorbance data from the UV–vis spectra of a set of solutions of DMPI with HP-β-CyD and β-CyD with mole fractions in the range of 0.0–1.0. Absorbance values were taken at a wavelength of λmax = 226 nm for all of the solutions at 298 K (Figs. 5b and 5d) . The top of the job curve correspond to the value of R (mole fraction of the guest) that provides the stoichiometry of the ICs formed; consequently, the ratio of guest and host is 1:2 for R ≈ 0.33, 1:1 for R ≈ 0.5, 2:1 for R ≈ 0.66 etc [46].

Here, the maxima of plots were found at R ≈ 0.5, indicating a 1:1 stoichiometry of both host–guest inclusion complexes (Figs. 5c and 5e) [47].

4.4. Association constant and thermodynamic parameters

Association or binding constants of DMPI with either HP-β-CyD or β-CD were calculated by UV–vis data. A part of ionic liquid based surfactant was inserted inside the truncated hydrophobic cavity of the both HP-β-CyD & β-CyD, so there was a significant variation in molar extinction coefficient (Δε) owing to the colour bearer part of the DMPI. The changes in absorbance (ΔA) of DMPI (226 nm) was studied against the concentration of β-CyD and its hydroxypropyl derivative at diverse

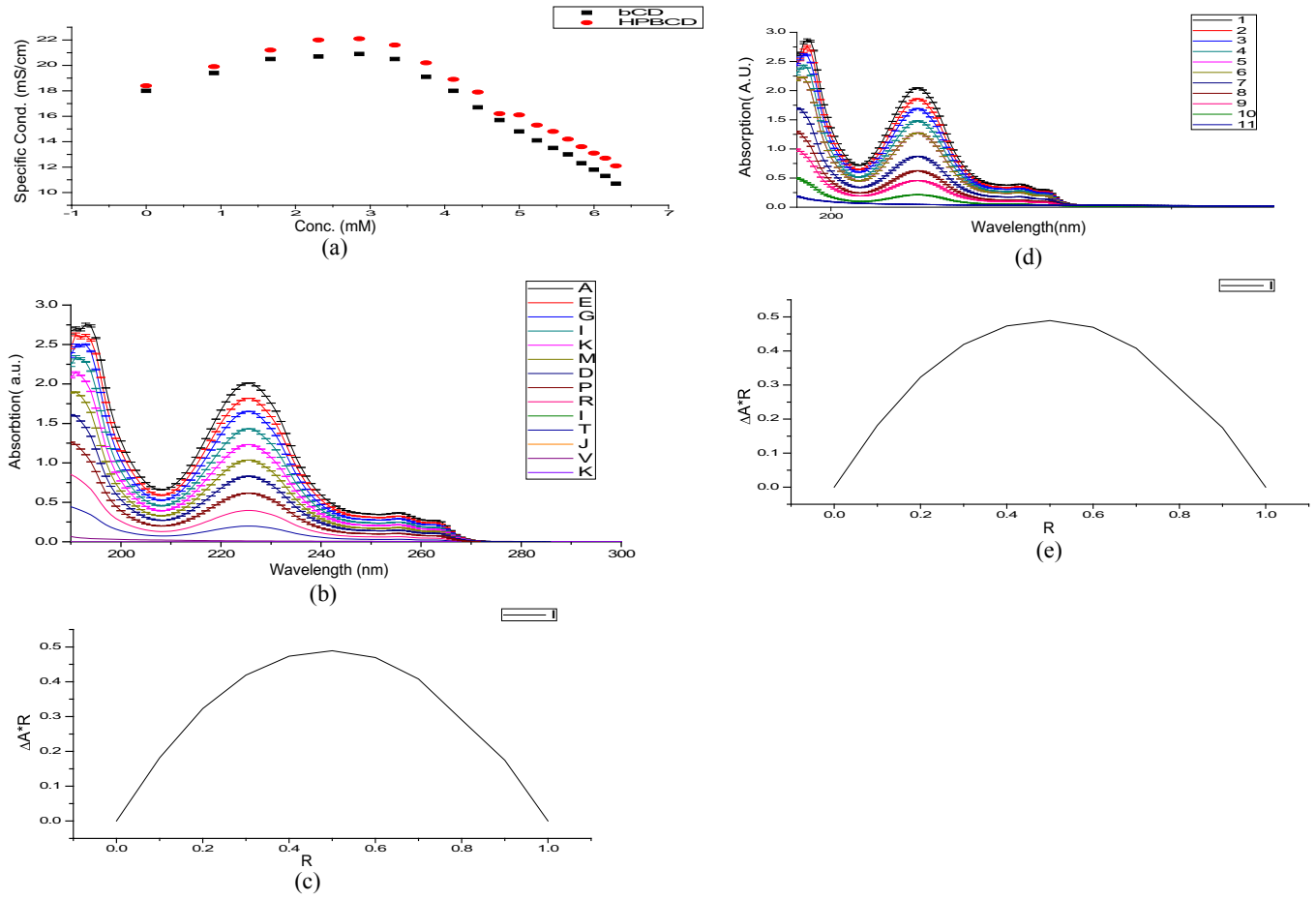

Fig. 5. (a) The variation of specific conductance of DMPI with respect to the concentration for HP-β-CyD at room temperatures (298 K). (b) and (c) Uv–vis graph (Plot with standard deviation data) & corresponding Job plot for DMPI and HP-β-CyD with maxima at 0.5; (d) & (e) Uv–vis graph (Plot with standard deviation data) & corresponding Job plot for DMPI and β-CyD with maxima at 0.5.

Table 2
The values of the association constants and the thermodynamic parameters obtained after analyzing UV–vis spectra.

	Temp/K_a	Ka/M^{-1}	ΔH^o/kJ mol^{-1}	ΔS^o/J $mol^{-1}K^{-1}$	ΔG^o/kJ mol^{-1}
HP-β-CyD	293	4.39×10^5	−44.85	265.23	−123.93
	298	1.47×10^6			
	303	2.11×10^6			
	308	1.71×10^6			
	313	1.73×10^6			
β-CyD	293	1.29×10^5	−20.304	28.00	−28.65
	298	0.93×10^5			
	303	1.045×10^5			
	308	0.681×10^5			
	313	0.782×10^5			

temperatures to establish the association constants (Ka).

The absorption values were used in the following Benesi-Hildebrand Eq. (1). (Benesi & Hildebrand, 1949) for the 1:1 host–guest complex formation.

$$\frac{1}{\Delta \mathbf{A}} = \frac{1}{\Delta\varepsilon[\mathbf{V}]\mathbf{Ka}} \times \frac{1}{[\mathbf{HP} - \beta - \mathbf{CyD}]} + \frac{1}{\Delta\varepsilon[\mathbf{V}]} \quad (1a)$$

$$\frac{1}{\Delta \mathbf{A}} = \frac{1}{\Delta\varepsilon[\mathbf{V}]\mathbf{Ka}} \times \frac{1}{[\beta - \mathbf{CyD}]} + \frac{1}{\Delta\varepsilon[\mathbf{V}]} \quad (1b)$$

Ka's values for both the systems were calculated from the ratio of intercept and slope of the straight line of double reciprocal plot (Table 2). [49,50] The thermodynamic parameters were derived rest on the association constants found at various temperatures with the help of van't Hoff equation Eq. (2).

$$\mathbf{lnKa} = -\frac{\boldsymbol{\Delta H^0}}{\boldsymbol{RT}} + \frac{\boldsymbol{\Delta S^0}}{\boldsymbol{R}} \quad (2)$$

On the basis of a linear correlation between $\ln K_a$ with 1/T in the above equation the thermodynamic parameters ΔH^o and ΔS^o for the formation of ICs may be obtained (Table 2) [51].

4.5. *From fluorescence spectroscopy: Further justification association parameter*

The predominant non covalent interaction of DMPI with CyDs was investigated by elegant spectrofluorimetry [52–54].

As shown in Scheme 1, Scheme 2, Figs. 1a, 1b, 1c, 2a, 2b, 3a, 3b, 3c,

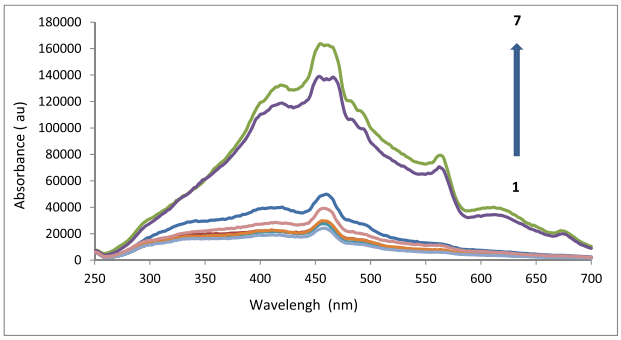

(a)

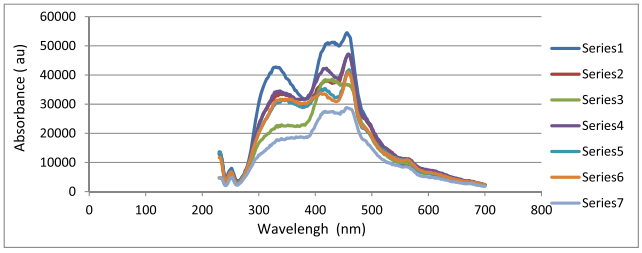

(b)

Fig. 6. (a): Fluorescence spectra of DMPI (50 μM) with different HP-β-CyD concentration (μM): 1) 20 μM 2) 30 μM, 3) 40 μM 4) 50 μM, 5) 60 μM, 6) 70 μM, 7) 80 μM. 6 (b): DMPI (50 μM) with different β-CyD concentration (μM): 7) 20 μM, 6) 30 μM, 5) 40 μM, 4) 50 μM, 3) 60 μM, 2) 70 μM, 1) 80 μM, obtained from the set of solution.

4, 5, 6, 7, 8a, 8b, 8c, 8d, 9 and 10, with an increase in the CyDs (HP-β-CyD & β-CyD) concentration, the DMPI showed enhanced fluorescence intensity with a slight hypsochromic shift of the emission peak [Tables S.7. a. and b.]. There was sudden decrease in the fluorescence spectral intensity in the mid concentration range, otherwise there was gradual increase. These findings certify the formation of DMPI-CyDs inclusion complexes. Molecules encapsulated inside CyD cavity often exhibit an increase in their fluorescence intensity. This is because the cyclodextrin's cavity offers a shielding microenvironment which can screen the excited singlet species from gradual quenching and non radiative decay process occurring in the aqueous solution [55,56].

Association or binding constants (Ka) of both the complexes were calculated from fluorescence data using the modified Benesi Hildebrand Eq. (3a) and (3b)

$$\frac{1}{[F-F_0]} = \frac{1}{[F'-F_0]\mathbf{K_a}} \times \frac{1}{[\mathbf{HP}-\beta-\mathbf{CyD}]} + \frac{1}{[F'-F_0]} \quad (3a)$$

$$\frac{1}{[F-F_0]} = \frac{1}{[F'-F_0]\mathbf{K_a}} \times \frac{1}{[\boldsymbol{\beta}-\mathbf{CyD}]} + \frac{1}{[F'-F_0]} \quad (3b)$$

[48]

Here F and F_0 represent the fluorescence intensities of DMPI in the presence and absence of either HP-β-CyD or β-CyD, Ka is the association constant of the complexation and F' signify fluorescence intensity when maximum DMPI molecules are effectively complexed with CyDs. The double reciprocal plots of $\frac{1}{[F-F_0]}$ vs. 1/[CyD] for surface active guest complexed with HP-β-CyD and β-CyD (shown in Figs. S.7.a and b) showed good linearity, implied the inclusion complexes had 1:1 stoichiometric ratio.

5. The thermodynamics of inclusion process

The Gibbs free energy ΔG for the binding of DMPI molecule to CyD cavity was calculated from the binding constant 'Ka' by using the following equation: **ΔG=- RT ln Ka**

The thermodynamic constant ΔG for the binding of DMPI molecule to HP-β-CyD and β-CyD were −20.6 and −18.8 kJ mol^{-1} respectively. The negative values of ΔG suggest, the inclusion process proceeded spontaneously at room temperature (298.00 K). The value of change in Gibbs free energy obtained from fluorimetric study was quite close to the same obtained from UV–vis spectra, especially in the case of β-CyD. Hydroxypropyl groups due to its free rotation around the single bonds probably make the entropy value very high in the case of HP-β-CyD inclusion complex. So we may say that it's a entropy driven process though ΔG value is not proportionately high as ΔS.

5.1. From surface tension

The graph of surface tension with respect to the logarithm of concentration for DMPI has shown in (Fig. S.8.a). From the graph, it was clear that at 4.44 mM concentration of HP-β-CyD one break point is present. The concentration is little less than the ideal concentration of 1:1 inclusion (i.e. 5 mM) as there may be less concentration of monomer DMPI due to its micellization. In case of host HP-β-CyD, the surface tension change was quite irregular with its gradual addition to water as it was more surface active compare to the β-CyD. HP-β-CyDs surface activity was more than β-CyD, probably due to the presence of propyl substitute with the cyclodextrin ring. (Fig. S.8.b).

5.2. From ^1H NMR

From the chemical shift values it was quite clear that shift of H3 & H5 is more than others proton in both the molecular host. So we may easily assume that inclusion was successfully happen between the both molecular hosts and the guest, DMPI. In solid inclusion complex the shift of $N(CH)_2$ was more than $N(+)CH_2(CH_2)_9$. So we may assume that methyl pyridinium part was inserted within the cavities of both hosts. Long chain hydrocarbon and methyl pyridinium part is attached to each other; we can expect 1:1 inclusion here [57].

At the same time it may also assume that long chain hydrocarbon was not inserted into the cavity of CyDs. Usually we get mixed mode of inclusion [both (1:1) and (2:1)] in the case of ion pair system with long chain hydrocarbon [22]. Aromatic part of the DMPI shown upfield shift, as it enters from hydrophilic to comparatively more hydrophobic region (comparatively more shielded region) (see Tables 3 and 4) (see Fig. 7).

Table 3
The values of chemical shifts δ (ppm) of pure DMPI(Guest) and in inclusion complex form.

Compound	$N+(CH)_2$ of pyridinium ring δ (ppm)	$N+(C)(CH)_2$ δ (ppm)	$N(+)CH_2$ δ (ppm)	$—CH_3$ group para to N δ (ppm)	$N(+)C(CH_2)_9$ δ (ppm)
DMPI	**8.713–8.697** (d)	**7.798–7.782(d)**	**4.522–4.485 (t)**	**2.509 (s)**	**1.201–1.046 (m)**
IC-1	**8.527–8.511** (d)	**7.762–7.746** (d)	**4.425–4.389 (t)**	**2.515 (s)**	**1.213–1.000 (m)**
Chemical Shift	**−0.186**	**−0.036**	**−0.097**	**0.006**	**−0.046**
IC-2	**8.530–8.513**(d)	**7.750–7.734** (d)	**4.433–4.397(t)**	**2.511 (s)**	**1.210–1.127(m)**
Chemical Shift	**−0.183**	**−0.048**	**−0.088**	**0.002**	**0.081**

Table 4
The values of chemical shifts δ (ppm) of pure cyclodextrins (HP-β-CyD and β-CyD) and in inclusion complex form.

Type of proton	Spin multiplicity	δ (ppm)		Spin multiplicity	**Shift (Δδ)**
		HP-β-CyD	DMPI/HP-β-CyD complex(IC-1)		
H-1	d	5.144–4.969	**5.098**		**−0.0415**
H-2	dd	3.504	**3.541–3.483**	**d**	**–**
H-3		3.908	**3.865**	**s**	**−0.043**
H-4		3.394	**3.325**	**s**	**–**
H-5	m	3.734	**3.702–3.621**	**m**	**0.222**
H-6	m	3.734	**3.702–3.621**	**m**	**–**
Type of proton	Spin multiplicity	δ (ppm)			**Shift (Δδ)**
		β-CyD	PDI/β-CyD complex(IC-2)		
H-1	d	4.923–4.932	**4.940–4.931**	**d**	**0.017**
H-2	dd	3.506	**3.565–3.512**	**m**	**–**
H-3	t	3.801–3.848	**3.758–3.735**	**t**	**−0.113**
H-4	t	3.419–3.466	**3.505–3.460**	**m**	**–**
H-5	m	3.706–3.766	**3.727–3.669**	**m**	**−0.097**
H-6	m	3.706–3.766	**3.727–3.669**	m	–

5.2.1. *From scanning electron microscopy (SEM) studies*

All SEM images were taken by conventionally after gold coating. SEM photographs of HP-β-CyD, DMPI and their inclusion complexes are shown in Figs. 8a–8d. Typical crystal of DMPI, and HP-β-CyD are found in many different sizes. Pure DMPI

appears as irregular-shaped crystal particles with large dimensions (Fig. 8a), HP-β-CyD shows in spherical particle type (Fig. 8b), and β-CyD crystallizes in polyhedral form [58]. The DMPI/HP-β-CyD inclusion complex shows as compact and surface-like structure crystal particles and is pretty unlike from the sizes and shapes of HP-β-CyD and DMPI (Figs. 8a–8c), which indicate the production of the inclusion complex. However, the DMPI/β-CyD inclusion complex appears as compact and homogeneous rod-like structure crystal particles and is also pretty different from the sizes and shapes of β-CyD and DMPI (Fig. 8d), which confirm the formation of the inclusion complexes. HP-β-CyD basically a kind of soft matter upon exposure to highly energetic electronic beam was deformed from its original structure. It was probably during electronic exposure static charge was accumulated in the exterior of HP-β-CyD, was mainly responsible for the structural deformation. Therefore extra precaution was taken during acquisition of the SEM images of the same compound. Finally we get better images by maintaining the voltage within 4 kV and acquire the pictures quickly. The SEM image of the pure β-CyD is available in another work carried out by our lab on same chemical by the same instrument (Also published in CPL, Elsevier, page 7, Fig. 6) [58].

5.2.2. *From EDS SEM*

SEM EDS is a qualitative method can be used to determine the structural features of raw materials, viz. CyDs and guest or the products prepared by diverse methods of preparation like physical mixture, solution complexation, co-evaporation and others [59,60]. Elemental composition analysis of all relevant samples was carried out qualitatively by using the EDS study and obtained graphical representation are shown in Fig. S.9.a–d. The elemental quantitative results were observed for C:O or C: N:O:I or C:O:I atomic ratios, which were fairly close to the expected bulk ratios indicating good distribution of the different species in the sample. Likewise Fig. S.9c–d, etc. show peaks corresponding to the iodine; it is direct evidence of the DMPI along with β-Cyd present in IC-1 & IC-2 both.

This noticeable observations reveal the minimum stoichiometric ratio of the different elements were maintained in all samples as well as inclusion complexes.

5.3. *Antibacterial study*

DMPI was shown significant antibacterial effect with gram negative bacteria E. Coli as expected [Fig. 9a–d] [61].

It may be assumed that pyridinium part was responsible for antibacterial property of the DMPI, so upon inclusion of this part, biological activity also should be reduced. We get expected result as the IC of the HP-β-CyD had shown less inhibition of the bacterial growth with all different concentration compare to the pure DMPI. So from this result we may conclude that the pure DMPI had more antibacterial effect compare to IC of the HP-β-CyD. Further, antibacterial property of IC of β-CyD will be explored in our future study with subsequent comparison with HP-β-CyD.

5.4. *From differential scanning calorimetry (DSC)*

From the Differential scanning calorimetry (DSC), varities of information such as crystallization, thermal stability, melting etc. can be obtained of chemical compounds [62].

The characteristic peaks of guest molecule in the thermogram may be completely diminished or shifted to the different temperatures due to the formation of inclusion complexes with the particular host [63].

Thermogram of solid guest, and ICs have been shown in the Fig. 10. DSC thermogram of DMPI shows a characteristic sharp distinct endothermic peak at 58 °C closely related to its melting point while in its ICs with both β-CyD and HP-β-CyD, comparatively flat and broadened signals are observed. These broad signals refer that there is a high loss of the crystallinity of DMPI in its ICs, indicating a strong complexation with CyDs and the peaks at higher temperature are probably due to the loss of water molecules adhered with ICs. As from the Fig. 10, it has been clearly seen that the nature of the peak at 58 °C in the thermogram for IC-2 (I.e. Complex of β-CyD & DMPI) is more flattened compare to that for the IC-1(i.e. Complex of HP-β-CyD & DMPI) which indicates more complexation of DMPI with β-CyD rather than with HP-β-CyD in the solid state.

5.5. *2D-ROESY SPECTRA analysis*

2D-ROESY NMR can confirm about successful inclusion by the appearance of intermolecular dipolar cross-correlations due to very close proximity of interacting protons [64,65]. If two protons are situated within 400 pm in space then they may produce rotating-frame NOE spectroscopy (ROESY) [66].

Inclusion event inside unique structure of β and HP-β-cyclodextrin cavity can be assertively shown by the appearance of NOE cross-peaks between the protons of cyclodextrin and the protons of the aromatic part of cationic surfactant identifying their spatial immediacy [67,68]. To prove successful inclusion here 2D-ROESY spectra of the complexes of DMPI with β and HP-β-cyclodextrin were recorded, which has confirmed the important correlation of aromatic protons of DMPI with H3 and H5 protons of β and HP-β-cyclodextrin (Fig. S.10), establishing inclusion of aromatic part of the DMPI.

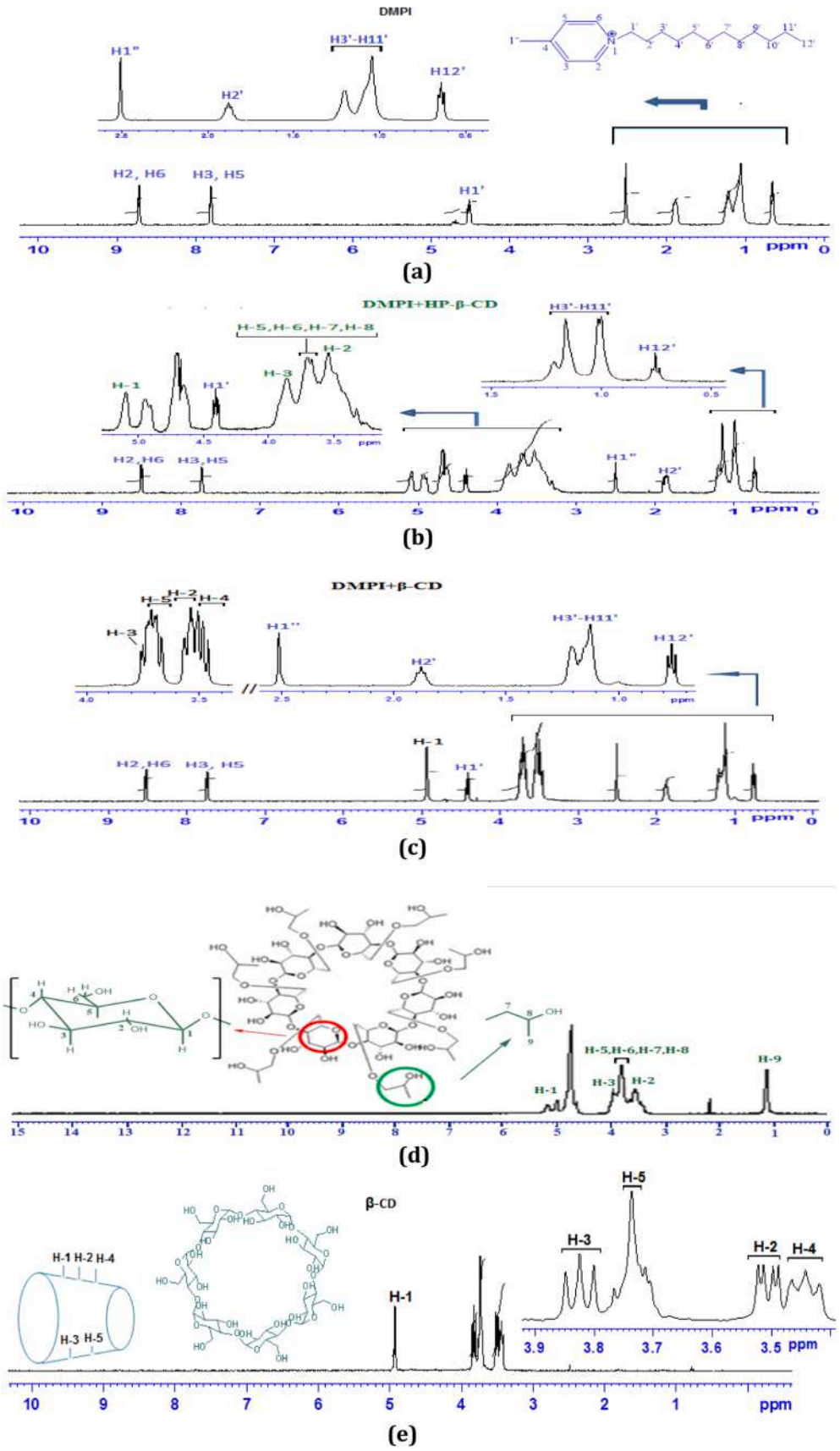

Fig. 7. a. FTNMR spectrum of DMPI. b. FTNMR spectrum of DMPI + HP-β-CyD inclusion complex (^{1}H) c. FTNMR spectrum of DMPI + β-CyD inclusion complex (^{1}H) d. FTNMR spectrum of HP-β-CyD e. FTNMR spectrum of HP-β-CyD.

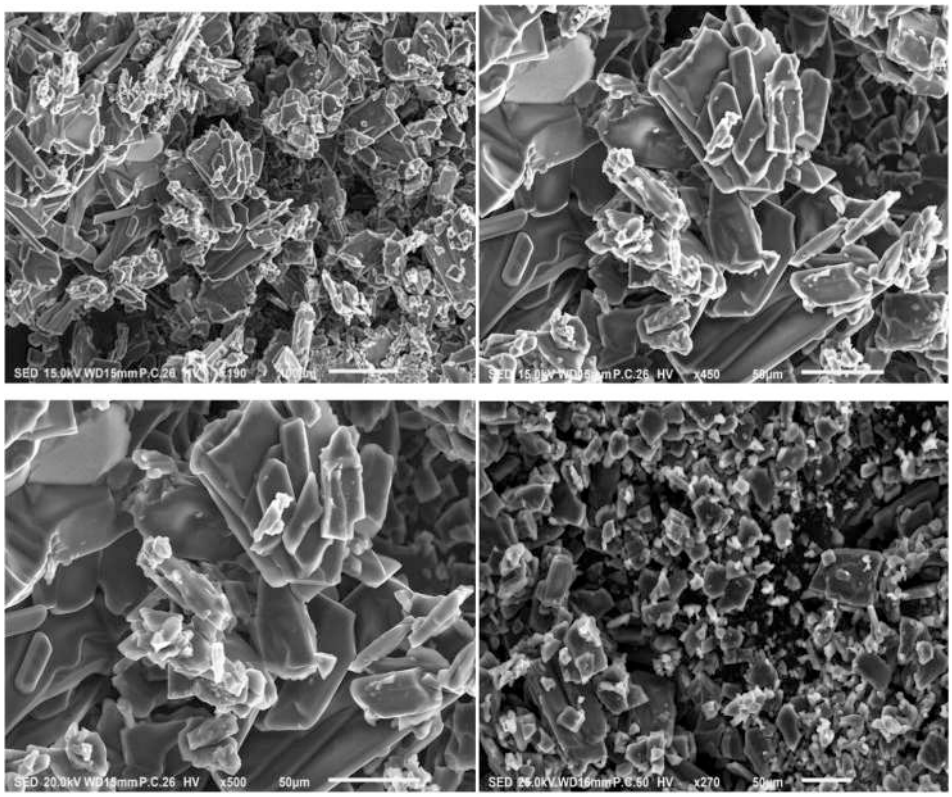

Fig. 8a. SEM images of the pure DMPI.

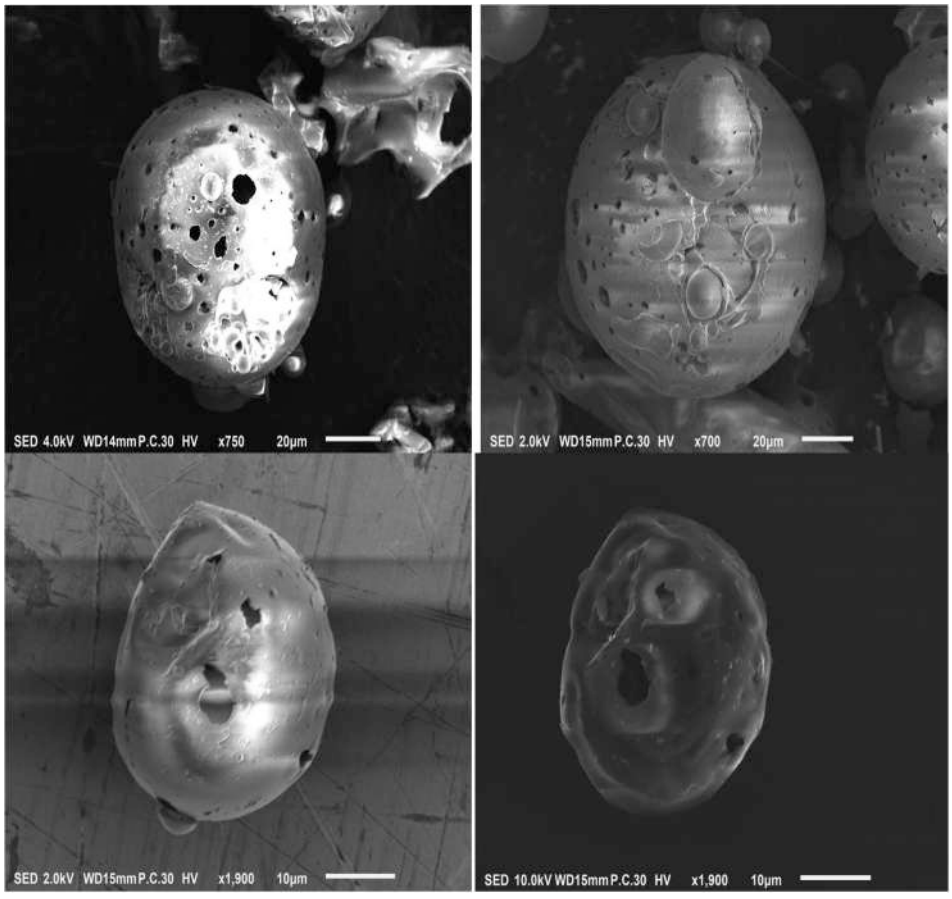

Fig. 8b. SEM images of the pure HP-β-CyD.

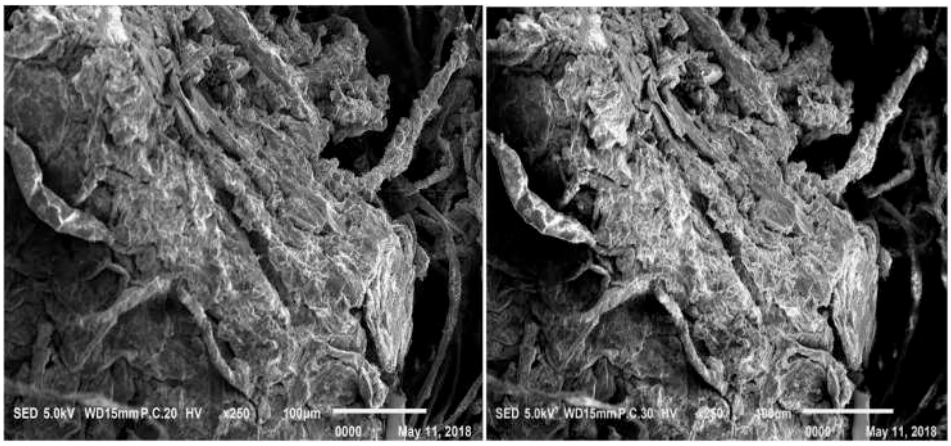

Fig. 8c. SEM images of the DMPI + HP-β-CyD inclusion complex.

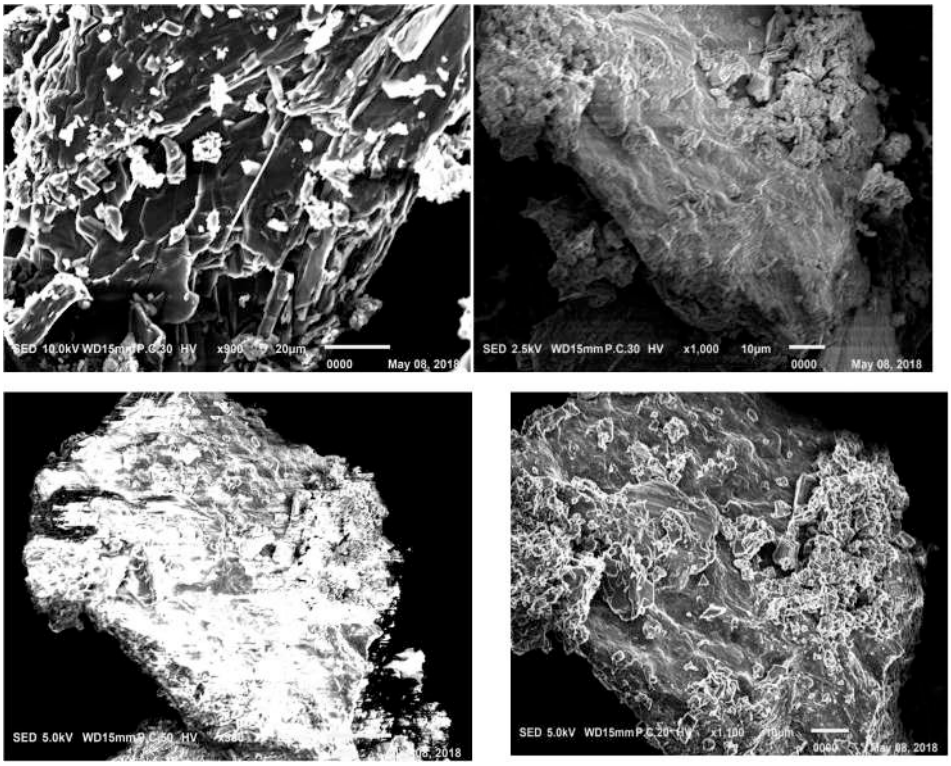

Fig. 8d. SEM images of the DMPI + β-CyD inclusion complex.

6. Conclusion

Characterisation of the compound confirms about its formation and the purity. Zeta potential values from DLS ensure about the stability of aqueous suspension of DMPI. Conductance and surface tension study between guest and host indicate the development of 1:1 inclusion complexes in aquous solution. Job plot obtained using the Uv–vis technique confirms the initial idea about the 1:1 mode of inclusion obtained from conductance and surface tension. FTIR, fluorescence & FTNMR experimental data insist us to propose that inclusion complexion occur more affectively in the case β-CyD than that of HP-β-CyD. SEM images have shown distinct changes in the surface morphology in the case β-CyD compare to HP-β-CyD. DSC data also support previous two experimental results. Anti bacterial effect was decrease more in case of the β-CyD + DMPI IC compare to the pure DMPI. One of the most valuable information from the 2D-ROESY is that, inclusion happened and through methyl substituted aromatic part of the surfactant. Association constant data from Uv–vis, fluorescence interestingly support stronger complexation of DMPI with HP-β-CyD rather than with β-CyD. In this regard, it may be concluded here that partial technique dependency (Only from uv–vis, fluorescence different trends were found & both were done in aqueous solution) makes it tricky to take strong and straightforward comparative decision, still this plenty of self supporting research data will help to enrich future research on ionic liquid surfactant and cyclodextrin research. It may also be resolute from major number of experimental observations that, the stronger inclusion complex were formed with ILBS viz. DMPI with the β-CyD compare to HP-β-CyD.

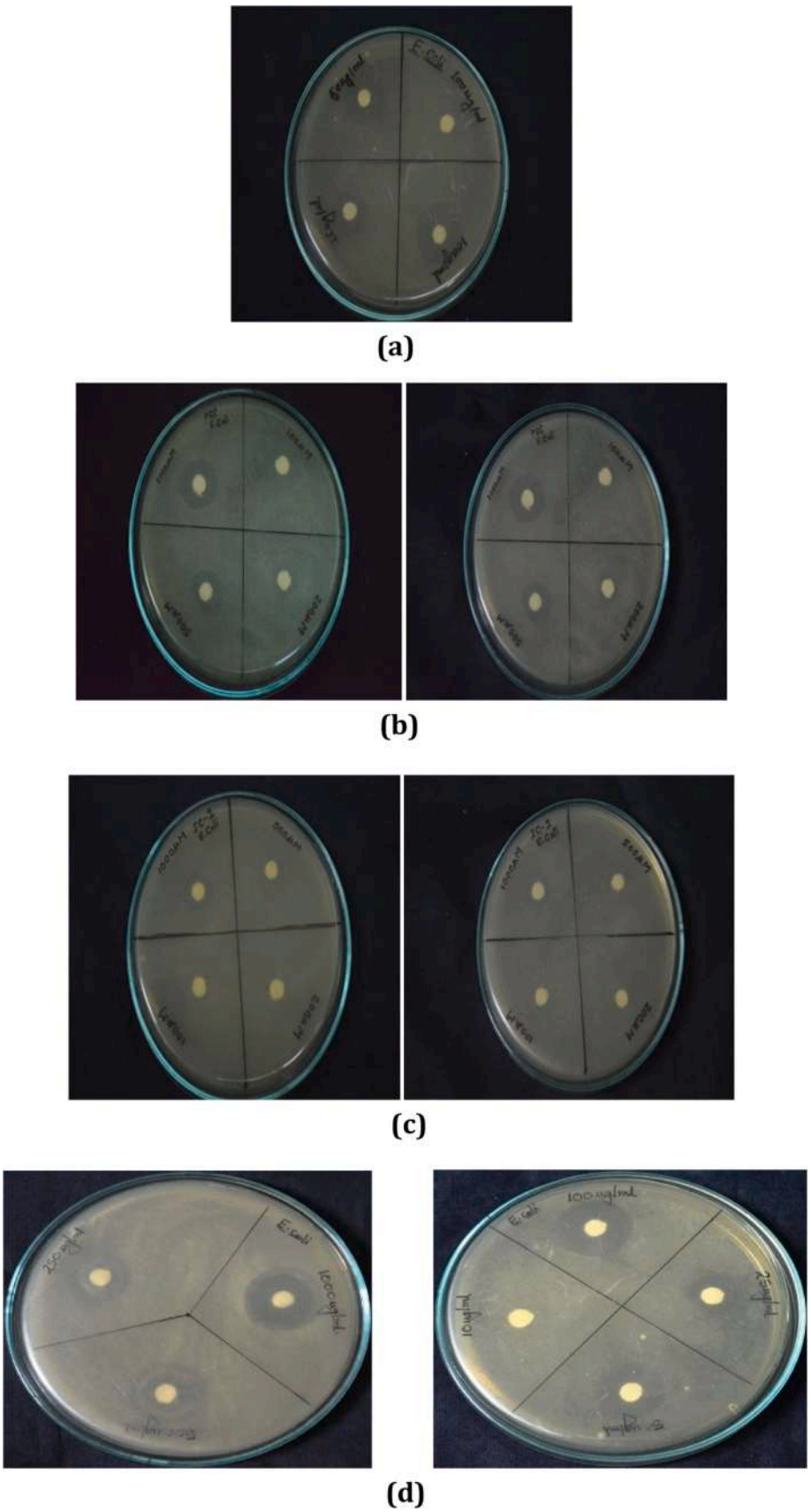

Fig. 9. Zone of inhibition against E. Coli by (a) Standard streptomycin (b) DMPI and (c) IC-1(Inclusion complex of HP-β-CyD and DMPI) (d) E. coli standard.

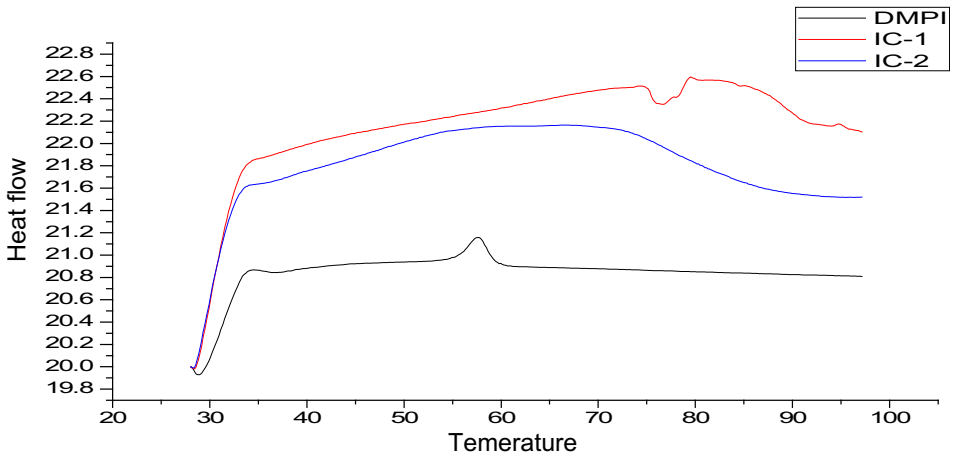

Fig. 10. DSC thermograms of solid DMPI and their ICs (IC-2 & IC-1 i.e. Complexes of β -CyD and HP-β-CyD respectively).

Declaration of Competing Interest

The authors declare that they have no known competing financial interests or personal relationships that could have appeared to influence the work reported in this paper.

Acknowledgements

Prof. (Dr.) Mahendra Nath Roy, is highly grateful to the UGC, New Delhi, Government of India for being awarded a onetime grant under Basic Scientific Research via the **Grant-in-Aid** no. **F.4-10/2010 (BSR)** concerning his brisk service for enhancement of research opportunities to facilitate further research activity. The authors are beholden for the Departmental **SAP DRS-III** under the University Grant Commission, New Delhi (no. **540/6/DRS/2007, SAP-1**), India, **RUSA** under **MHRD**, Government of India and Chemistry Department, the University of North Bengal for financial assistance and instrumental aids in order to carry on this research work. We delightedly avouch NEHU, SAIF for furnishing the excellent FT-NMR & ESI-MS facility. The authors concede Prof. S. K. Saha for his constant guidance in the research of surfactant chemistry related parts and Prof. Pranab Ghosh, Chemistry, N.B.U. for his kind cooperation to execute the 300 MHz ^{1}H NMR allied with this paper. Authors also like to acknowledge Mr. Rajib Sarkar (Head in charge, USIC, NBU) and **specially** to **Dr. Tamal Sarkar** (DEPT. OF HIGH ENERGY, NBU) for SEM analysis and Mr. **Priyankar Roy** (Research Scholar ,Botany, NBU) for anti bacterial study. The authors also acknowledge Dr. Soumen Bhattacharjee & his scholar Dr. Tanmoy Dutta for GC-MS facility, Mr. Abhisek Saha, Mrs. Beauty Mahato for their supports.

Appendix A. Supplementary material

Supplementary data to this article can be found online at https://doi.org/10.1016/j.cplett.2021.138401.

References

[1] K.N. Marsh, J.A. Boxall, R. Lichtenthaler, Room temperature ionic liquids and their Mixtures-a review, Fluid Phase Equilib. 219 (2004) 93–98.
[2] J. Doupont, R.F. De Souza, P.A.Z. Suarez, Ionic liquid (molten salts) phase organometallic catalysis, Chem. Rev. 102 (2002) 3667–3692.
[3] T. Welton, Room-temperature ionic liquids. Solvents for synthesis and catalysis, Chem. Rev. 99 (1999) 2071–2084.
[4] M.J. Earle, J.M.S.S. Esperanca, M.A. Gilea, J.N. Canongia Lopes, L.P.N. Rebelo, J. W. Magee, K.R. Seddon, J.A. Widegren, The distillation and volatility of ionic liquids, Nature 439 (2006) 831–834.
[5] J.D. Holbrey, K.R. Seddon, The phase behaviour of 1-alkyl-3-methylimidazolium tetrafluoroborates; ionic liquids and ionic liquid crystals, J. Chem. Soc., Dalton Trans. (1999) 2133–2139.
[6] C.P. Fredlake, J.M. Crosthwaite, D.G. Hert, S.N.V.K. Aki, J.F. Brennecke, Thermophysical Properties of Imidazolium-Based Ionic Liquids, J. Chem. Eng. Data 49 (2004) 954–964.
[7] L. Gaillon, J. Sirieix-Plenet, P. Letellier, J. Solut. Chem. 33 (2004) 1333–1347.
[8] P.D. Galgano, O.A. El Seoud, Surface-Active Ionic Liquids: Syntheses, Solution Properties, and Applications, in: J. Mun, H. Sim (Eds.), Handbook of Ionic Liquids: Properties, Applications and Hazards, Nova Publisher, Hauppauge, 2012, pp. 521–548.
[9] J. Valentino, STELLA AND QUANREN HE, Cyclodextrins, Toxicol. Pathol. 36 (2008) 30–42.
[10] Subhadeep Saha, Aditi Roy, Kanak Roy & Mahendra Nath Roy, Study to explore the mechanism to form inclusion complexes of β-cyclodextrin with vitamin molecules, Sci. Rep. 6, 35764.
[11] M.N. Anjana, C. Sreeja, Jipnomon Joseph Nair, an updated review of cyclodextrins-an enabling technology for challenging pharmaceutical formulations, Int. J. Pharm. Pharmaceut. Sci. 5 (3) (2013). ISSN- 0975-1491.
[12] Kanak Roy, Pranish Bomzan, Milan Chandra Roy, Mahendra Nath Roy, Inclusion of tyrosine derivatives with α-cyclodextrin in aqueous medium of various pH conditions by surface tension, conductance, UV–Vis and NMR studies, J. Mol. Liq. 230 (2017) 104–112.
[13] D. Meha Hiral, P. Prabhakara Akhilesh, J.V. Kamath, Enhancement of Solubility by Complexation with Cyclodextrin and Nanocrystallisation, Int. Res. J. Pharm. 3 (5) (2012) 2230–8407.
[14] A.C. Illapakurthy, Y.A. Sabnis, B.A. Avery, M.A. Avery, C.M. Wyandt, Interaction of Artemisinin and Its Related Compounds with Hydroxypropyl-*b*-cyclodextrin in Solution State: Experimental and Molecular-Modeling Studies, J. Pharmaceut. Sci. 92 (3) (2003).
[15] Sarah Gould, Robert C. Scott, 2-hydroxypropyl-b-cyclodextrin (HP-β-CD): A toxicology review, Food Chem. Toxicol. 43 (2005) 1451–1459.
[16] O. Robert, Williams, Vorapann Mahaguna, Mongkol Sriwongjanya, Characterization of an inclusion complex of cholesterol and hydroxypropyl-b-cyclodextrin, Eur. J. Pharm. Biopharm. 46 (1998) 355–360.
[17] Niloy Roy, Raja Ghosh, Koyeli Das, Debadrita Roy, Tulika Ghosh, Mahendra Nath Roy, Study to synthesize and characterize host-guest encapsulation of antidiabetic drug (TgC) and hydroxy propyl-β-cyclodextrin augmenting the antidiabetic applicability in biological system, J. Mol. Struct. 1179 (2019) 642–650.
[18] Longxiao Liu, Suyan Zhu, Preparation and characterization of inclusion complexes of prazosin hydrochloride with β-cyclodextrin and hydroxypropyl-β-cyclodextrin, J. Pharm. Biomed. Anal. 40 (2006) 122–127.
[19] Y. Francois, et al., Determination of aqueous inclusion complexation constants and stoichiometry of alkyl(methyl)-methylimidazolium-based ionic liquid cations and neutral cyclodextrins by affinity capillary electrophoresis, J. Sep. Sci. 30 (2007) 751–760.
[20] G. Gouhier, et al., Ionic liquids and cyclodextrin inclusion complexes: limitation of the affinity capillary electrophoresis technique, Anal. Bio. Chem. 408 (28) (2016) 8211–8220, https://doi.org/10.1007/s00216-016-9931-z.
[21] Mitali Kundu, Mahendra Nath, Roy, Preparation, interaction and spectroscopic characterization of inclusion complex of a cyclic oligosaccharide with an antidepressant drug, J. Incl. Phenom. Macrocycl. Chem. 89 (2017) 177–187.
[22] Raja Ghosh, Deepak Ekka, Biplab Rajbanshi, Ananya Yasmin, Mahendra Nath Roy, Synthesis, characterization of 1-butyl-4-methylpyridinium lauryl sulfate and its inclusion phenomenon with β-cyclodextrin for enhanced applications, Colloids Surf. A 548 (2018) 206–217.
[23] Soumik Bardhan, Kaushik Kundu, Bidyut K. Paul, Swapan K. Saha, Interfacial composition and characterization of a quaternary water-in-oil mixed surfactant (cationic of different alkyl chain lengths + polyoxyethylene type nonionic) microemulsions in absence and presence of inorganic salts, Colloids and Surfaces A: Physicochem, Eng. Aspects 433 (2013) 219–229.
[24] Amritaa Mitra, Anand Pariyar, Suranjana Bose, Pinaki Bandyopadhyay, Arindam Sarkar, First phenalenone based receptor for selective iodide ion sensing, Sens. Actuat. B 210 (2015) 712–718.

[25] Tanusree Ray, Deepak Ekka, Milan Chandra Roy and Mahendra Nath Roy, Exploration of Host Guest Inclusion Complex of β-CD with an Ionic Liquid ([C_4mpy]Cl) in Aqueous Media by Physicochemical Approach, Chem Sci Rev Lett. 4 (14) (2015) 619–629.

[26] Mahendra Nath Roy, Binoy Chandra Saha and Kalipada Sarkar, Physico-chemical studies of a biologically active molecule (L-valine) predominant in aqueous alkali halide solutions with the manifestation of solvation consequences, Phys. Chem. Liq. 53 (6) (2015) 785–801.

[27] G. Chakraborty, M.P. Chowdhury, S. Bardhan, S.K. Saha, Surface activity and modifying effects of 1-Naphthol, 2-Naphthol and2,3-Dihydroxynaphthalene on self-assembled nanostructures of 1-Hexadecyl-3-methylimidazolium chloride, Colloids Surf. A 516 (2017) 262–273.

[28] Biplab Roy, Pritam Guha, Ravi Bhattarai, Prasant Nahak, Gourab Karmakar, Priyam Chettri and Amiya Kumar Panda, Influence of Lipid Composition, pH, and Temperature on Physicochemical Properties of Liposomes With Curcumin as Model Drug, J. Oleo Sci. 65 (5) (2016) 399–411.

[29] M. Katcka, T. Urbanski, Infrared absorption spectra of quaternary salts of, Bulletin de l'Académie polonaise des sciences. Série des sciences chimiques XII (1964) 615–621.

[30] R.B. Viana, A.B.F. da Silva, A.S. Pimentel, Adsorption of sodium dodecyl sulfate on Ge substrate: the effect of a low-polarity solvent, Int. J. Mol. Sci. 13 (2012) 1–14. https://doi.org/10.1155/2012/903272.

[31] C.N. Banwell, E.M. McCash, Fundamental of Mol, Spec. Tata McGraw-Hill, New Delhi, 2009.

[32] J.G. Weers, D.R. Scheuing, Structure/performance relationships in monoalkyl/dialkyl cationic surfactant mixtures, J. Colloid Interface Sci. 145 (2) (1991) 563–580.

[33] P. Saad, C.R. Flach, R.M. Walters, R. Mendelsohn, Infrared spectroscopic studies of sodium dodecyl sulphate permeation and interaction with stratum corneum lipids in skin, Int. J. Cosmet. Sci. 34 (2012) 36–43.

[34] J.B. Lambert, H.F. Shurvell, D.A. Lightner, R.G. Cooks, Macmillan Publishing Company., Introduction to Organic Spectroscopy, Macmillan Publ., New York, 1987.

[35] Bojidarka Ivanova, Michael Spiteller, Water, Air, Soil Pollution, Article number: 1918 (2014), 225.

[36] Y. Ishihama, H. Katayama, N. Asakawa, Surfactants usable for electrospray ionization mass spectrometry, Anal. Biochem. 287 (1) (2000 Dec 1) 45–54, https://doi.org/10.1006/abio.2000.4836. PMID: 11078582.

[37] Priyankar Dey, Sandipan Ray, Mousumi Poddar Sarkar, Tapas Kumar Chaudhuri, Chemical characterization and assessment of antioxidant potentiality of Streptocaulon sylvestre Wight, an endangered plant of sub-Himalayan plains of West Bengal and Sikkim, BMC Complem. Altern. Med. 15 (1) (2015) 107.

[38] www.chem.ucla.edu/~bacher/UV-vis/uv_vis_tetracyclone.html.html (Accessed on 26/11/18).

[39] Robert W. Newberry, Ronald T. Raines, The n→ π* Interaction, Acc. Chem. Res. 50 (8) (2017) 1838–1846.

[40] American Society for Testing and Materials, ASTM Standard D 4187-8, Zeta Potential of Colloids in Water and Waste Water, 1985.

[41] R.J. Hunter, Zeta Potential in Colloid Science: Principles and Applications, Academic Press, UK, 1988.

[42] B. Derjaguin, L. Landau, Theory of the stability of strongly charged lyophobic sols and of the adhesion of strongly charged particles in solutions of electrolytes, Acta Physico Chemica URSS 14 (1941) 633.

[43] E.J.W. Verwey, J.Th.G. Overbeek, Theory of the stability of lyophobic colloids, Elsevier, Amsterdam, 1948.

[44] P. Job, Formation and Stability of Inorganic Complexes in Solution, Ann. Chim. 9 (1928) 113–203.

[45] Subhadeep Saha, Aditi Roy, and Mahendra Nath Roy, Mechanistic Investigation of Inclusion Complexes of a Sulfa Drug with α- and β-Cyclodextrins, Ind. Eng. Chem. Res. 56 (41) (2017) 11672, https://doi.org/10.1021/acs.iecr.7b02619.

[46] J.S. Renny, L.L. Tomasevich, E.H. Tallmadge, D.B. Collum, Method of Continuous Variations: Applications of Job Plots to the Study of Molecular Associations in Organometallic Chemistry, Angew. Chem. Int. Ed. 52 (2013) 11998–12013.

[47] J.V. Caso, L. Russo, M. Palmieri, G. Malgieri, S. Galdiero, A. Falanga, C. Isernia, R. Iacovino, Investigating the Inclusion Properties of Aromatic Amino Acids Complexing beta-Cyclodextrins in Model Peptides, Amino Acids 47 (2015) 2215–2227.

[48] H.A. Benesi, J.H. Hildebrand, A spectrophotometric investigation of the interaction of iodine with aromatic hydrocarbons, J. Am. Chem. Soc. 71 (1949) 2703–2707.

[49] Y. Dotsikas, E. Kontopanou, C. Allagiannis, Y.L. Loukas, Interaction of 6-*p*-toluidineylnaphthalene-2-sulphonate with *β*-cyclodextrin, J. Pharm. Biomed. Anal. 23 (2000) 997–1003.

[50] M.N. Roy, A. Roy, S. Saha, Probing inclusion complexes of cyclodextrins with amino acids by physicochemical approach, Carbohydr. Polym. 151 (2016) 458–466.

[51] Y. He, X. Shen, Interaction between *β*-cyclodextrin and ionic liquids in aqueous solutions investigated by a competitive method using a substituted 3H-indole probe, J. Photochem. Photobiol., A 197 (2008) 253–259.

[52] C.N. Sanrame, R.H. Rossi, G.A. Arguello, Effect of β-cyclodextrin on the excited state properties of 3-substituted indole derivatives, J. Phys. Chem. 100 (1996) 8151–8156.

[53] A. Orstan, J.B. Rossi, 2739–2745 Investigation of the. beta.-cyclodextrin-indole inclusion complex by absorption and fluorescence spectroscopies, J. Phys. Chem. 91 (1987).

[54] S. Prabu, M. Swaminathan, K. Sivakumar, R. Rajamohan, Preparation, characterization and molecular modeling studies of the inclusion complex of Caffeine with Beta-cyclodextrin, J. Mol. Struct. 1099 (2015) 616–624.

[55] Q. Zhang, Z. Jiang, Y. Guo, R. Li, Complexation study of brilliant cresyl blue with β-cyclodextrin and its derivatives by UV–vis and fluorospectrometry, Spectrochim. Acta Part A Mol. Biomol. Spectrosc. 69 (2008) 65–70.

[56] Min Zhang, Jinxia Li, WeipingJia, Jianbin Chao, Liwei Zhang, Theoretical and experimental study of the inclusion complexes of ferulic acid with cyclodextrins, Supramol. Chem. 21 (2009) 597–602.

[57] Subhadeep Saha, Mahendra Nath Roy, Probing supramolecular complexation of cetylpyridinium chloride with crown ethers, J. Mol. Struct. 1147 (2017) 776–785.

[58] Niloy Roy, Pranish Bomzan, Mahendra Nath Roy, Probing Host-Guest inclusion complexes of Ambroxol Hydrochloride with α-& β-Cyclodextrins by physicochemical contrivance subsequently optimized by molecular modeling simulations, Chem. Phys. Lett. 748 (2020) 137372, https://doi.org/10.1016/j.cplett.2020.137372.

[59] D.R. de Araujo, S.S. Tsuneda, C.M.S. Cereda, F.D.G.F. Carvalho, P.S.C. Preté, S. Fernandes, et al., Development and pharmacological evaluation of ropivacaine-2-hydroxypropyl-β-cyclodextrin inclusion complex, Eur. J. Pharm. Sci. 33 (1) (2007) 60–71.

[60] D. Duchêne, Cyclodextrins and their industrial uses, Editions de Santé, Paris, 1987.

[61] Z. Baker, R.W. Harrison, B.F. Miller, The bactericidal action of synthetic detergents, J. Exp. Med. 74 (6) (1941) 611.

[62] M.N. Roy, S. Saha, M. Kundu, S. Saha, S. Barman, Exploration of inclusion complexes of neurotransmitters with β-cyclodextrin by physicochemical techniques, Chem. Phys. Lett. 43 (2016) 655.

[63] L.R. Teixeira, R.D. Sinisterra, R.P. Vieira, A. Scarlatelli-Lima, M.F. Moraes, M. C. Doretto, H. Beraldo, An inclusion compound of the anticonvulsant sodium valproate into α-cyclodextrin: Physico-chemical characterization, J. Incl. Phenom. Macrocycl. Chem. 54 (1–2) (2006) 133–138.

[64] B. Yang, J. Lin, Y. Chen, Y. Liu, Artemether/hydroxypropyl-beta-cyclodextrin host-guest system: characterization, phasesolubility and inclusion mode, Bioorg. Med. Chem. 17 (2009) 6311–6317.

[65] A.C. Servais, A. Rousseau, M. Fillet, K. Lomsadze, A. Salgado, J. Crommen, B. Chankvetadze, Capillary electrophoretic and nuclear magnetic resonance studies on the opposite affinity pattern of propranolol enantiomers towards various cyclodextrins, J. Sep. Sci. 33 (11) (2010) 1617–1624.

[66] Isabelle Correia, Nabil Bezzenine, Nello Ronzani, Nicole Platzer, Jean-Claude Beloeil, Bich-Thuy Doa, Study of inclusion complexes of acridine with β- and (2, 6-di-O-methyl)-β-cyclodextrin by use of solubility diagrams and NMR spectroscopy, J. Phys. Org. Chem. 15 (2002) 647–659.

[67] T. Ishizu, C. Hirata, H. Yamamoto, K. Harano, Structure and intramolecular flexibility of β-cyclodextrin complex with (−)-epigallocatechin gallate in aqueous solvent, Magn. Reson. Chem. 44 (2006) 776–783.

[68] B. Rajbanshi, S. Saha, K. Das, B.K. Barman, S. Sengupta, A. Bhattacharjee, M. N. Roy, Study to Probe Subsistence of Host-Guest Inclusion Complexes of α and β-Cyclodextrins with Biologically Potent Drugs for Safety Regulatory Dischargement, Sci. Rep. 8 (1) (2018 Aug 29) 13031.